Proceedings Paper:
Zhang, F., Zhou, S. and Martsinovich, N. orcid.org/0000-0001-9226-8175 (2025) Molecular-modified dyes for dye-sensitised solar cells (DSSCs): a computational chemistry investigation. In: Journal of Physics: Conference Series. 2024 4th International Conference on Advanced Materials and Chemical Engineering (AMCE 2024), 25-27 Oct 2024, Guangzhou, China. IOP Publishing

https://doi.org/10.1088/1742-6596/2961/1/012029

Journal of Physics:
Conference Series

PAPER • **OPEN ACCESS**

Molecular-modified dyes for Dye-sensitised solar cells (DSSCs): a computational chemistry investigation

To cite this article: Fan Zhang *et al* 2025 *J. Phys.: Conf. Ser.* **2961** 012029

Molecular-modified dyes for Dye-sensitised solar cells (DSSCs): a computational chemistry investigation

Fan Zhang *[1], Shijie Zhou [2] and Natalia Martsinovich [1]

[1] The University of Sheffield, Sheffield, South Yorkshire, S3 7HF, UK
[2] Jiangsu University, Zhenjiang 212013, Jiangsu, China

* Corresponding author's e-mail: fanzhang19@foxmail.com

Abstract: Dye-sensitised solar cells (DSSCs) are of great potential for science development to solve the problem of energy crisis. The sensitizers (dyes) for DSSCs are explored and discussed in this project. Computational chemistry investigations based on Gaussian 09 are carried out to determine the computational data of dye molecules and to deduce their properties. Light absorptions, molecular orbitals, and energy levels of dyes are specifically explored and discussed. Molecular structures are modified diversely to achieve better features. The new dye molecule with better properties is successfully designed.

1. Introduction

With the problems of global industrialization, overpopulation, and climate change, the world is suffering from an unprecedented energy crisis. The worldwide energy demand is expected to double by the year 2050 and triple by the end of the century [1]. An abundant supply of energy is necessary for global political, economic, and environmental stability. Conventional energy sources like coal, oil, and gas are faced with great challenges due to their limited reserves. Such kinds of growing concerns have urged humans to do more research on clean, efficient, and renewable energy sources [2]. Solar energy is such a kind of ideal source and has been widely used in the field of electricity generation. The key to the breakthrough of solar energy is to improve the efficiency of its conversion to electrical energy [3].

Scientists have been devoting themselves to developing low-cost, highly efficient, and environmentally friendly solar cells (photovoltaic cells). Dye-sensitized solar cells (DSSCs) have provided a new approach to the booming development of solar cells [4]. Compared with traditional silicon cells, dye-sensitized solar cells are much more promising due to their relatively high conversion efficiency, which has reached up to 14% and is still rising, together with many other unique superiorities [5].

DSSC was first invented by O'regan and Grätzel from the use of a mesoporous TiO_2 electrode in 1991 [6]. Grätzel and Hagfeldt also made great progress in revealing the principle of DSSC in 1995, resolving a certain number of mysteries concerning its working mechanism at that time [7].

2. Structure and materials of DSSCs

The research of Grätzel and Hagfeldt attracted focus from different fields. Following the research findings, scientists gradually revealed the conceptual structure of DSSC with its working principle [8-9]. One DSSC consists of a photoelectric anode, a mesoporous semiconductor film (usually nanocrystalline TiO_2, or other metal oxide nanomolecules), a light-absorbing "dye" (photo-sensitizer), an electrolyte/hole transporter, and a counter-electrode (photoelectric anode) [4, 10]. It shows a

characteristic "sandwich" structure. When exposed to the light, the dye absorbs the photon and becomes photoexcited. An electron is then donated to an electron-accepting nano-crystalline (usually TiO_2). Afterward, the dye is regenerated by a redox reaction of the dye cation with a redox couple (electrolyte), while the electron donated by the dye moves to the external electric circuit to generate electrical power [11]. The structure and the mechanism are depicted in Figure 1. The specific energy levels and electron transfer processes in DSSC are depicted in Figure 2.

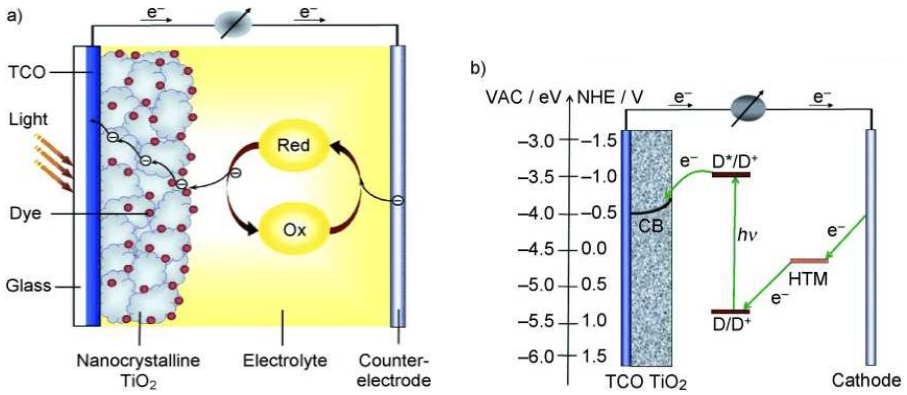

Figure 1. Structure and mechanism of DSSC (left) and energy levels and electron transfer processes in DSSC (right) [TCO: transparent conducting oxide (electrode)] [11].

Materials used for DSSC have been upgraded over the past decades, with most of the development focusing on dyes and nanostructured metal oxides. TiO_2, served as the mesoporous semiconductor film in the earliest DSSC structure, has always been the major material for the composition of DSSC due to its remarkable stability, nontoxicity, and semi-conductivity [4, 12]. Following the treatment of TiO_2, Grätzel and O'regan [6] managed to use $TiCl_4$ in 1993 to improve the quality of TiO_2 nanoparticles [13]. Apart from TiO_2, ZnO is another metal oxide semiconductor used in DSSC since its microscopic structures (bandgap and conduction band edge) are quite similar to those of TiO_2 [4]. Despite its relatively poor stability, ZnO has higher electron mobility than TiO_2, which makes it favor electron transport [4, 12]. According to the research of Keis et al. in 2000 and Nguyen et al. in 2009, the efficiency of ZnO has been increased by up to 6.6% by improvements in its structure [14, 15]. Furthermore, it is reported that metal oxides such as SnO_2, In_2O_3, Zn_2SnO_4, $SrTiO_3$, and Nb_2O_5 have been treated in DSSC as mesoporous electron-accepting nanocrystalline materials in recent years [16-18].

Apart from nanostructured metal oxides, the sensitizer (dye) is another crucial part of DSSC. To contribute to remarkable and effective abilities of energy conversion, a good photo-sensitizer has to fulfill the following features [4]:

(i) A wide-range light absorption covering the whole visible region;

(ii) A strong ability to bind to the semiconductor surface (TiO_2);

(iii) Operating an efficient electron transfer from the dye molecule to the semi-conductor, and avoiding the reversed transfer;

(iv) A rapid process of regeneration by the redox couple;

(v) Necessary photochemical, electrochemical, and thermal stabilities.

The typical structure of an organic dye molecule is shown in Figure 2. The lowest unoccupied molecular orbital (LUMO), known as the "acceptor" part in charge of the directional electron transfer, is mainly localized on the anchoring group next to the TiO_2 semiconductor. The high-occupied molecular orbital (HOMO), known as the "donor" part, is mainly delocalized away from the semiconductor. A π-conjugated "bridge" that controls the light absorption properties of the molecule is between the donor and the acceptor. These three parts consist of a basic "donor-bridge-acceptor" structure, which is also known as a "D-B-A" or "D-π-A" structure [4, 10, 11].

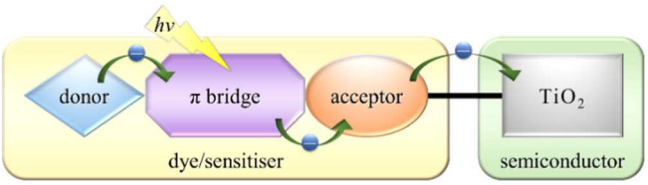

Figure 2. The basic structure of dye molecule.

To achieve a dye molecule with better features and qualities, different parts of the molecule can be modified and analyzed [19]. This project aimed to calculate the electronic and optical properties of diverse dyes, analyze their computational chemistry based on calculated data, and design new dyes with better properties.

3. Computational methods

All calculations were implemented in the Gaussian 09 package. The basic structure of the dye molecule explored in this computational project is shown in Figure 3 and Table 1. By commenting on differences among the features of six molecules (C209, C210, C213, C214, C215, and C216) and comparing them with the literature data, a relatively ideal molecule could be selected [19]. Further explorations were then carried out by changing the donor, π-bridge, and acceptor into diverse groups. A final dye molecule with the best properties would be deduced after a series of analyses.

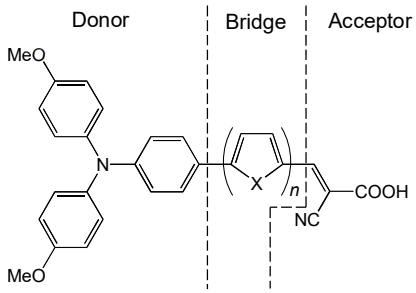

Figure 3. The basic structure of dye molecules explored in this project.

Table 1. Representation of Element X and Number *n* in Figure 3.

Molecules	X	*n*
C209	O	1
C210	O	2
C213	S	1
C214	S	2
C215	Se	1
C216	Se	2

For each molecule, the optimization, molecular orbitals (MOs) simulation, and UV-Vis absorption spectra simulation were operated via the software. The molecules were calculated both in a vacuum and under the environment of the solution (chloroform in this project). Settings for these calculations are listed in Table 2 [19, 20].

Table 2. Settings for calculations in Gaussian 09.

	Optimizations	MO simulations	UV-Vis absorption spectra
Job type	Optimization	Energy	Energy
Method	Ground state / DFT /	Ground state / DFT /	TD-SCF / DFT /

	Default spin / B3LYP	Default spin / B3LYP	Default spin / CAM-B3LYP
Basis set	6-31G(d)	6-31G(d)	6-31G(d)
Other settings	–	Checkpoint file: Default name	Solution for more states; Replacement of 6 with 25
Solvation settings (for calculation in solution)	Model: CPCM Solvent: Chloroform	Model: CPCM Solvent: Chloroform	Model: CPCM Solvent: Chloroform

Energies of molecular orbitals (HOMO and LUMO in particular) were exported after the calculation. Images of MOs were visualized and saved. The data and the spectra of UV-Vis absorption were also exported for further analyses.

4. Results and discussions

Detailed data simulated from computational calculations were rather complicated, and hence only key results were shown in tables and figures below for discussion.

4.1. Calculations on basic dye molecular structures

Six basic molecules listed in Figure 3 and Table 1 were calculated, and the key data of HOMO-LUMO energy gaps were listed in Table 3. The unit of energy was transferred into electron volt (eV) from the initial atomic unit (a.u.), of which 1 a.u. equals 27.211 eV [20]. The λ_{max} data of UV-Vis absorption spectra are listed in Table 4.

Table 3. Key data of HOMO-LUMO energy gaps (in eV).

	C209	C210	C213	C214	C215	C216
In vacuum	2.62	2.33	2.50	2.23	2.49	1.94
In solution	2.50	2.22	2.34	2.08	2.35	1.82
Lit. values [19]	2.42	2.12	2.33	2.03	2.30	1.97

Table 4. λ_{max} of UV-Vis absorption spectra (in nm).

	C209	C210	C213	C214	C215	C216
In vacuum	408.01	439.92	540.13	449.54	425.52	488.46
In solution	555.84	561.14	540.13	485.71	463.40	528.57
Lit. values from [19]	482	504	485	518	500	553

As was shown from the calculated data, the values of energy gaps followed the order: C209 > C213 > C215 > C210 > C214 > C216. However, the values of λ_{max} data followed the reversed order. Considering the differences between molecular structures, it could be indicated that the elongation of the π-conjugated linker (the "bridge" structure) leads to a decrease in the value of energy gaps and an increase in the UV peaks. To summarise, by comparing the experimental data with the literature, it could be deduced that the calculation generally performed well despite a little deviation. Both C214 and C216 molecules showed a particularly successful prediction. Considering the differences between sulfur and selenium, C214 was a more ideal material for dyes and would be further explored in the rest of the project.

4.2. General analyses on C214 molecule

The molecular structure, molecular orbital, and UV-Vis spectrum of the C214 molecule were depicted in Figures 4, 5, and 6 to make comparisons.

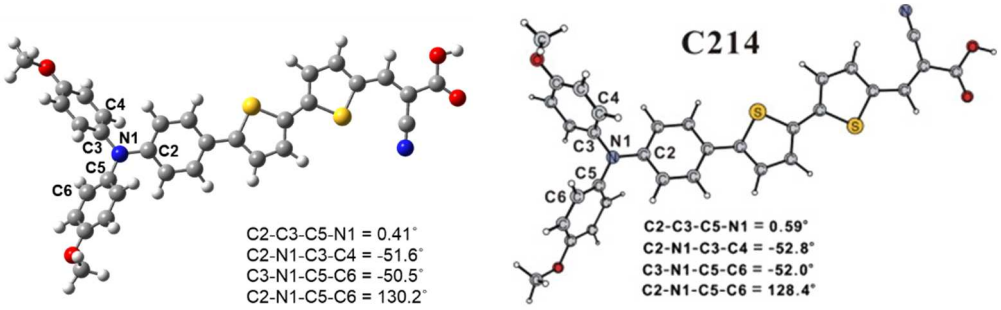

Figure 4. Experimental structure optimization of C214 and the dihedral angle (left) compared with the literature one (right).

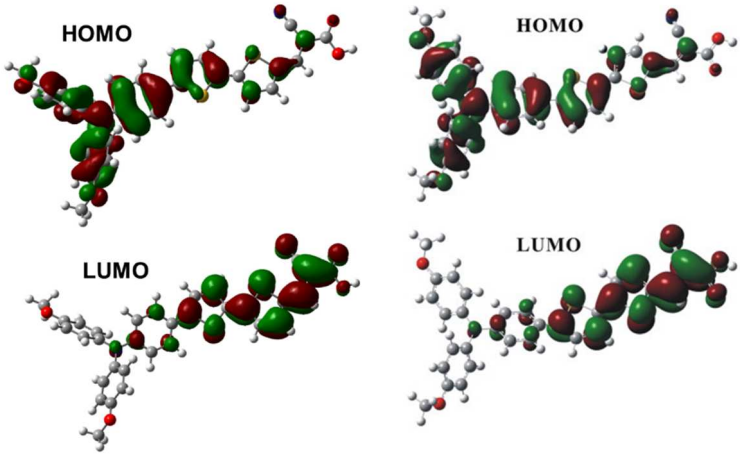

Figure 5. Experimental molecular orbitals of C214 (left) compared with the literature ones (right).

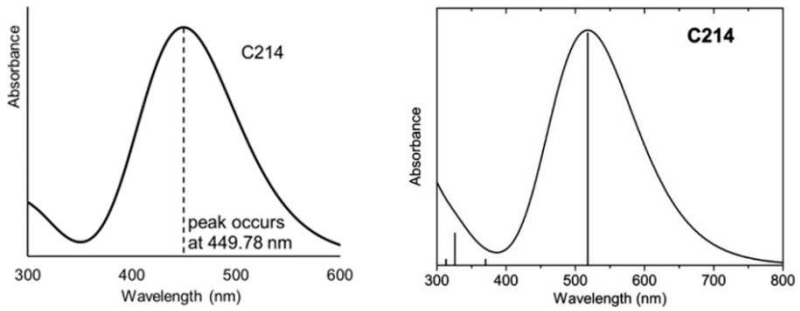

Figure 6. Experimental UV-Vis spectrum of C214 (left) compared with the literature one (right).

As was depicted, the molecular structures and the dihedral angles after the optimization were almost the same for both experimental and literature ones, and so were MO plots. As expected, the HOMO electron cloud density was mainly distributed on the donor and the bridge part, while the LUMO was mainly on the acceptor part. This ensured an efficient HOMO-LUMO electron transfer as depicted in Figure 2.

4.3. Modifications on the acceptor group of C214

The effect of modifying the acceptor group was explored by changing two initial groups [cyano group (−CN) and carboxylic group (−COOH)] into others. It could be indicated from the result that the energy gaps of modified molecules were either increased or decreased. Also, the UV-Vis absorption ranges became either wide or narrow, with the corresponding peaks moving towards either higher or lower wavelengths.

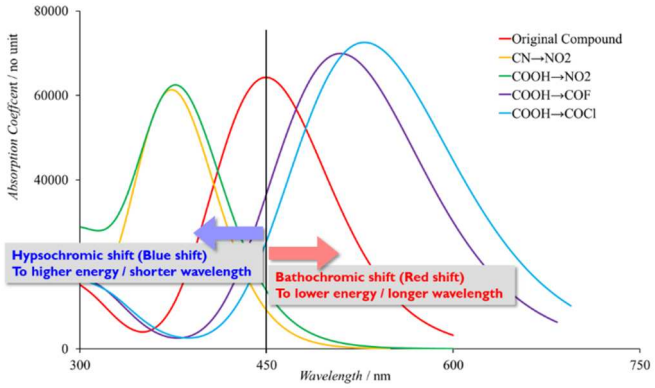

Figure 7. UV-Vis spectra of molecules with acceptors modified.

Figure 7 shows the UV-Vis absorption spectra of diverse molecules after changing the acceptor groups. Two molecules (blue and purple curves in the diagram) showed a wider range of absorption, with their peaks shifting to lower energy / longer wavelength. This phenomenon was called "bathochromic shift" or "red shift" since it moved closer to red light in the visible light range [20, 21]. The other two molecules (yellow and green curves in the diagram) showed a reversed feature, which was called "hypsochromic shift" or "blue shift" [20, 21].

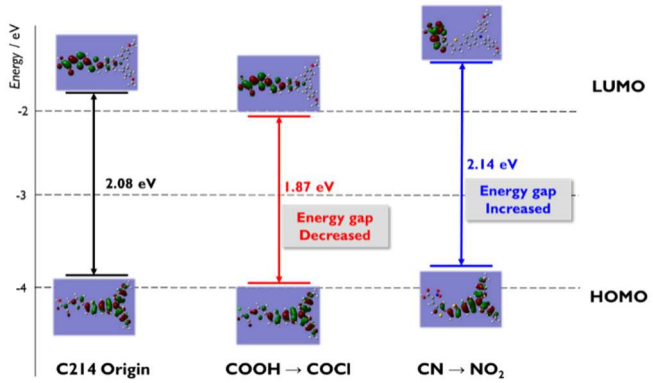

Figure 8. Molecular orbitals and HOMO-LUMO energy levels.

Figure 8 depicts the molecular orbitals and HOMO-LUMO energy levels of two typical modified molecules and the original one. It was not difficult to discover that for the HOMO, the energy levels changed slightly; but for the LUMO, the change was obvious. This was because of the modification on the acceptor group where the LUMO electron cloud density is mainly distributed [22]. For the molecule whose energy gap decreased to 1.87 eV, it was observed from the electron cloud images that the border between HOMO and LUMO was not as obvious as the original one. Both HOMO and LUMO were distributed on the π-conjugated part to a certain extent, which would benefit the HOMO-LUMO electron transfer. This further accounted for the redshift of the molecule as mentioned above, since the main source of maximum light absorptions for most sensitizers came from HOMO-LUMO electron transfer [10].

A photo-sensitizer needs to be efficient by owning a wide-range light absorption that covers the visible region as much as possible [4]. With the features discussed above, it can be deduced that the modification of changing the carboxylic group into an acyl chloride group (COOH → COCl, blue curve in Figure 7) is an ideal perfection for the acceptor group.

4.4. Modifications on the donor group of C214

The effect of modifying the donor group was explored by changing various parts of donors into others.

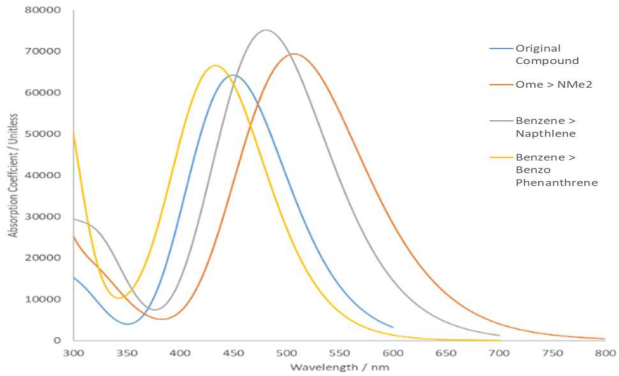

Figure 9. UV-Vis spectra of molecules with donors modified.

Figure 9 shows the UV-Vis absorption spectra of diverse molecules after modifying the donor groups. The molecule with two OMe groups changed into two NMe_2 groups (orange curve in the diagram) showed an ideal wider range of absorption, with its peak shifting to lower energy / longer wavelength. Another molecule with benzene changed into naphthalene (grey curve in the diagram) also showed a redshift. However, the best modification on the donor was to change OMe into NMe_2, because it covered almost the whole region of visible light with a peak wavelength of more than 500 nm, which is beneficial to both absorption and electron transfer.

4.5. Modifications on the π-conjugated bridge of C214

The effect of modifying the π-conjugated bridge was explored by changing the bridge part of C214 (two thiophene groups) into other groups.

When analyzing the data on energy levels and gaps, it was observed that only the molecule with three thiophene groups [thiophene (3)] showed a lower gap. In specific, thiophene (3) showed a slightly lower LUMO energy and a slightly higher HOMO energy, due to the increased atom numbers that influenced conjugation effects [22]. By comparing its MO diagram with the initial molecule [thiophene (2)], thiophene (3) showed less overlap (Figure 10).

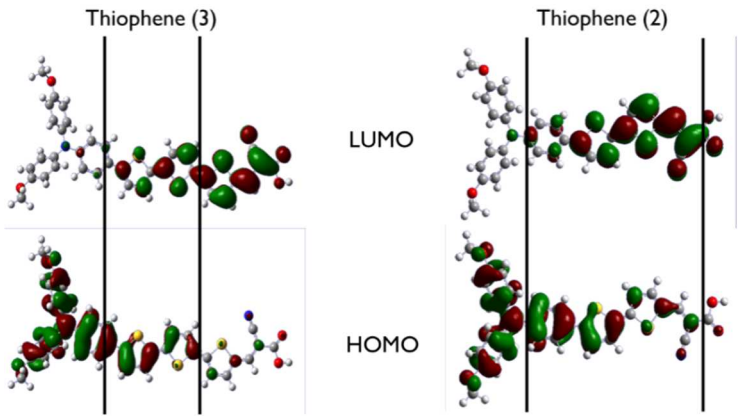

Figure 10. MO diagrams for thiophene (3) and thiophene (2).

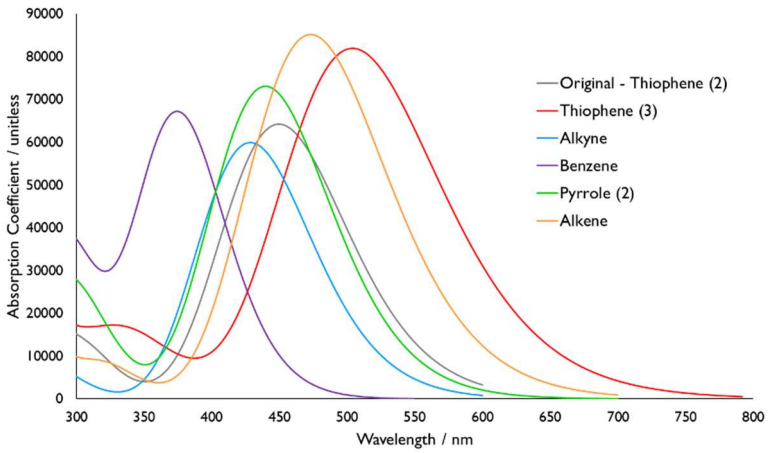

Figure 11. UV-Vis spectra of molecules with the bridge modified.

Figure 11 shows the UV-Vis absorption spectra of diverse molecules after changing the bridge group. Thiophene (3) showed a wider range of absorption, with an obvious red shift of its peak. It could be deduced that the best modification on the bridge was to add one thiophene group.

4.6. The effect of changing the solvents

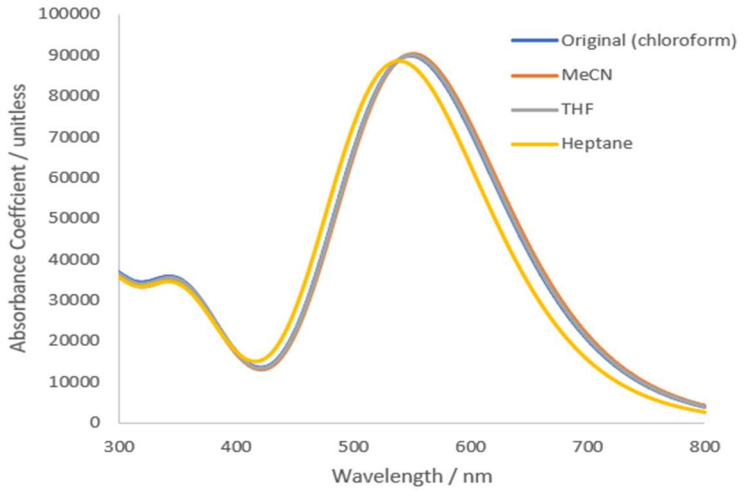

Figure 12. UV-Vis spectra with solvents modified.

The dye molecule was also tested in alternative solvents, acetonitrile, tetrahydrofuran, and heptane, to explore the effect of changing the solvents. The UV-Vis absorption spectra were shown in Figure 12, indicating the differences between each molecule were small, which meant the effect of changing solvents was minimal.

5. Conclusions

A dye molecule with the best features should make the most of ideal modifications in each different part. By summarizing the discussions above, the best molecule structure can be determined, based on the original C214 structure with three alternations made: (i) acceptor: changing CN into COCl; (ii) donor: changing OMe into NMe_2; (iii) bridge: three thiophene groups.

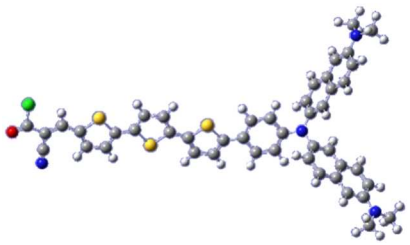

Figure 13. Structure of the designed dye molecule.

The dye with better properties was successfully designed (Figure 13). The light absorption of this dye would cover the majority of the visible range, with a good "red shift" of the peak wavelength. Theoretically, it would show good qualities of both light absorption and electron transfer and would largely improve the efficiency of energy conversion for solar cells. Explorations on semiconductors shown in Figure 2 can be carried out for future computational or experimental works and can be compared with this project to achieve integrated research on DSSCs.

References

[1] Mascaretti L., Chen Y., Henrotte O., Yesilyurt O., Shalaev V., Naldoni A., & Boltasseva A. *ACS Photonics*, 2023, **10 (12)**, 4, 079-103.
[2] Abdellah I., Eletmany M., & El-Shafei A. *Materials Today Communications*, 2023, **35**, 106, 170.
[3] Mohsin M., Ishaq T., Bhatti I., Maryam, Jilani A., Melaibari A., & Abu-Hamdeh N. *Nanomaterials*, 2023, **13 (3)**, 546.
[4] Hagfeldt A., Boschloo G., Sun L., Kloo L., & Pettersson H. *Chemical Reviews*, 2010, **110**, 6, 595-663.
[5] Alizadeh A., Roudgar-Amoli M., Bonyad-Shekalgourabi S., Shariatinia Z., Mahmoudi M., & Saadat F. *Renewable and Sustainable Energy Reviews*, 2022, **157**, 112, 047.
[6] O'regan B. & Grätzel M. *Nature*, 1991, **353**, 737.
[7] Hagfeldt A. & Grätzel M. *Chemical Reviews*, 1995, **95**, 49-68.
[8] Hagfeldt A. & Grätzel M. *Accounts of Chemical Research*, 2000, **33**, 269-77.
[9] Grätzel M. *Nature*, 2001, **414**, 338-344.
[10] Agasti A., Peedikakkandy L., Kumar R., Mohanty S., Gondane V., & Bhargava P. *Springer Handbook of Inorganic Photochemistry*, Springer, Berlin, 2022.
[11] Mishra A., Fischer M., & Bäuerle P. *Angewandte Chemie International Edition*, 2009, **48**, 2, 474-99.
[12] Zhang T., He Q., Yu J., Chen A., Zhang Z., & Pan J. *Nano Energy*, 2022, **104**, 107, 918.
[13] Nazeeruddin M., Kay A., Rodicio I., Humphry-Baker R., Müller E., Liska P., Vlachopoulos N., & Grätzel M. *Journal of the American Chemical Society*, 1993, **115**, 6, 382-90.
[14] Keis K., Lindgren J., Lindquist S., & Hagfeldt A. *Langmuir*, 2000, **16**, 4, 688-94.
[15] Nguyen H., Mane R., Ganesh T., Han S., & Kim N. *The Journal of Physical Chemistry C*, 2009, **113**, 9, 206-09.
[16] Ali J., Bibi S., Jatoi W., Tuzen M., Jakhrani M., Feng X., & Saleh T. *Materials Today Communications*, 2023, 106, 840.
[17] Bykkam S., Prasad D., Maurya M., Sadasivuni K., & Cabibihan J. *Sustainability*, 2021, **13 (14)**, 7, 685.
[18] Yahya M., Bouziani A., Ocak C., Seferoğlu Z., & Sillanpää M. *Dyes and Pigments*, 2021, **192**, 109, 227.
[19] Chen S., Yang L., & Li Z. *Journal of Power Sources*, 2013, **223**, 86-93.
[20] Agnello S. *Spectroscopy for Materials Characterization*, Wiley, New York, 2021.
[21] Barone V., Alessandrini S., Biczysko M., Cheeseman J., Clary D., McCoy A., DiRisio R., Neese F., Melosso M., & Puzzarini C. *Nature Reviews Methods Primers*, 2021, **1 (1)**, 38.
[22] Roohi H. & Mohtamadifar N. *RSC Advances*, 2022, **12 (18)**, 11, 557-73.